

GROUND SURFACE RESPONSE TO THE TRANSPORT LOADS IN THE TUNNEL REINFORCED WITH A THREE-LAYER LINING

Svetlana Girmis¹, Vitaliy Ukrainets¹, Larisa Gorshkova¹,*Olga Vyshar¹ and Fariza Auesheva¹

¹ Faculty of Architecture and Construction, Toraighyrov University, Kazakhstan

*Corresponding Author, Received: 04 Aug. 2024, Revised: 08 Oct. 2024, Accepted: 09 Oct. 2024

ABSTRACT: Based on mathematical modelling, effective methods have been developed for studying the dynamics of tunnels under transport loads (from an object moving through the tunnel). For a tunnel with a circular three-layer lining, such a method has only been developed in the case of a deep-buried tunnel. This article focuses on a similar shallow-buried tunnel, modeled as a circular cylindrical three-layer shell, composed of a thick middle layer (filler) and thin outer layers (cladding), embedded in an elastic half-space. The horizontal boundary of the half-space (the ground surface) is parallel to the shell axis. The motion of the filler and the half-space is described by the dynamic equations of elasticity theory in Lamé potentials, while the motion of the cladding layers – by the classical equations of shell theory. The equations are represented in a moving coordinate system associated with a uniformly moving load along the inner surface of the shell. Based on the obtained solution and numerical experiments, the stress-strain state of the ground surface was investigated under the influence of a transport normal load acting symmetrically relative to the vertical diametral plane of the tunnel on the three-layer steel-concrete lining, as well as when the intensity of one of its symmetric halves was doubled. This asymmetric load distribution leads to significant changes in the displacements and stresses of the ground surface, with horizontal displacements increasing by more than an order of magnitude. Thus, the transport load must be symmetrical in the operation of shallow-buried tunnels in urban areas.

Keywords: Tunnel, Elastic half-space, Three-layer shell, Transport load, Stress-strain state.

1. INTRODUCTION

The engineering of shallow tunnels has the effect of reducing both the cost and the time required for construction. Nevertheless, the operational experience of such tunnels in urban areas demonstrates a notable surge in the intensity of vibrations in buildings and structures located in close proximity to their route, predominantly attributable to transport loads. It can be reasonably deduced that exceeding the permissible norm level of vibrations established for buildings will result in their unsuitability for habitation. Furthermore, the vibrations have an adverse impact on a number of high-precision technological processes and on human health. In light of these considerations, it is imperative to ensure the adequate reliability of all components of the underground structure, while concurrently addressing the issue of permissible proximity to surface structures [1].

Consequently, the study of the dynamics of tunnels subjected to transport loads represents a significant engineering challenge, which is addressed through the application of a modeling research approach. The primary models employed to investigate the dynamics of tunnels subjected to transport loads are those pertaining to the dynamic behavior of an elastic half-space (the first problem) or elastic space (the second problem) with a reinforced extended cavity undergoing movement along its axis. The first problem deals with the

dynamics of a shallow tunnel, whereas the second problem considers the dynamics of a deep tunnel. The question of the permissible proximity of buildings and structures to shallow tunnels can be addressed by investigating the first problem. Once the second problem has been solved, it is possible to determine the distance from the tunnel at which the impact effect of transport loads on the surrounding massif will be insignificant. This will allow recommendations to be made regarding the optimal depth of its embedment [2].

The widespread use of closed circular cylindrical homogeneous and multilayered shells in tunnel structures raises the issue of studying elastic media with cylindrical cavities of circular cross-section. The model transportation problem, as it pertains to a circular deep tunnel, was previously considered in [3, 4] and numerous other papers. This problem concerns the effect of a transport load moving with constant velocity on an infinitely long circular cylindrical thick-walled or thin-walled homogeneous shell in elastic space. A comparable issue was addressed in the context of a multilayered (three-layer or two-layer) shell comprising rigidly interconnected concentric layers with different physical and mechanical properties, as discussed in [5 – 7]. In [5], the stress-strain state (SSS) of a three-layer elastic shell (with a thick middle layer and thin outer layers) was studied; in [6], the SSS of a two-layer elastic shell (with a thick inner layer and a thin outer layer); and in [7], the SSS of a two-layer

elastic shell (with a thin inner layer and a thick outer layer), with the SSS of the elastic medium surrounding these shells also analyzed. In all these articles, the motion of the thin shell layers was described by the classical equations of shell theory, while the motion of the thick layers and the surrounding elastic medium was described using the dynamic equations of elasticity theory in vector form.

In the case of shallow tunnels, the solution to the model transportation problem becomes significantly more complex due to the notable deformation of the ground surface and its impact on the stress concentration in the surrounding area of the structure during the diffraction of reflected waves. The number of scientific works published on this issue is relatively limited, particularly [8 – 18]. Articles [8 – 17] examine the effect of a moving load on a circular cylindrical homogeneous shell located in an elastic half-space. In article [8], the motion of the shell under the influence of a uniformly moving load of an arbitrary type was described by the classical equations of shell theory, while in article [9], the dynamic equations of elasticity theory in vector form were used, which were also used to describe the motion of the elastic half-space. Numerical studies were conducted to analyze the effect of a moving normal load on the shell. In articles [10 – 12], a similar problem to [8] was examined, but under the influence of uniformly moving loads of various types: axial tangential load [10], axial tangential and normal loads [11], as well as torsional and normal loads [12].

In works [13, 14], a closed-form semi-analytical solution is presented for vibrations caused by a moving point load in a tunnel reinforced with a homogeneous lining embedded in a half-space. The tunnel lining is modeled as an elastic hollow cylinder, while the surrounding ground is treated as a linear viscoelastic material. The total wave field in the half-space with a cylindrical cavity is represented by outgoing cylindrical waves and downward-propagating plane waves. Unlike [13, 14], article [15] investigates the vibrations of the same tunnel in an elastic half-space subjected to uniformly distributed dynamic pressure. Assuming plane strain, the equations of motion for the tunnel lining and the surrounding medium are reduced to two wave equations in polar coordinates using Helmholtz potentials.

In article [16], an analytical method is presented for calculating ground vibrations from a tunnel in a multilayered half-space. Using the transfer matrix method, the dynamic matrix of the system is obtained for multilayered soil overlying a half-space or bedrock. The tunnel is coupled with the multilayered soil through transformations between cylindrical and plane waves. The proposed method provides a highly efficient tool for predicting

vibrations caused by underground railways.

In article [17], a new two-dimensional (2D) semi-analytical method is proposed for calculating ground vibrations from a tunnel located in a homogeneous half-space with an irregular surface. The circular tunnel is represented as an elastic body, while the soil is modeled as an elastic, isotropic, and homogeneous half-space with an irregular surface. A virtual horizontal interface is introduced to divide the soil domain into an irregular section with an arbitrary surface shape and a half-space with a circular cavity. The scattered wave field from the irregular surface is modeled using a boundary integral equation.

The effect of a moving load on a circular cylindrical two-layer shell situated in an elastic half-space, whose model was presented in [6], is examined in [18].

In this paper, the structure of shallow tunnel lining is modeled as an extended circular cylindrical shell consisting of three concentric layers: a thick middle layer (filler) and thin outer layers (cladding). It is assumed that the contact between the shell and the surrounding medium, as well as between the layers of the shell, is rigid.

Due to the widespread use of three-layer shell linings in tunnel construction in recent years [19], and the lack of adequate dynamic calculations for such structures and the ground surface above them under transport loads, the research conducted in this paper is both important and timely.

The study conducted in this article differs from the earlier research on a deep tunnel reinforced with a three-layer lining [5] in that it takes into account the impact of waves reflected from the Earth's surface, which arise under transport loading, on the tunnel and the surrounding soil mass, and also includes the calculation of the SSS of the Earth's surface. Accounting for this effect leads to more accurate results in calculating the SSS of the tunnel lining and the surrounding soil mass compared to [5].

The objective of the research:

- to provide an analytical solution to the problem and to develop computer programs based on this solution to study the dynamics of a shallow tunnel supported by a three-layer lining, corresponding to the model adopted in this paper, under stationary transport loads;

- to numerically investigate the SSS of the ground surface under the influence of various types of transport loads on the three-layer tunnel lining.

The problem formulation and solution are outlined in the Results section. In the same section, the results of the numerical experiments are presented and subsequently analyzed in the Discussion section. The methodology employed in the study is delineated in the Methods section. The Conclusion section presents a synthesis of the findings from the research project.

2. RESEARCH SIGNIFICANCE

The solution obtained and the computer programs developed on its basis permit the study of the dynamics of the rock body and the ground surface along the route of a tunnel supported by a three-layer lining at varying depths of embedment and different speeds of transport for loads of various types. The speed and type of transport loads exert a significant influence on the dynamics of the ground surface. This must be taken into account, for example, in the construction of subways, especially in light of the current era of rapid growth in high-speed rail transport. By selecting the appropriate materials and thicknesses for the tunnel lining layers at a given shallow depth, it is possible to reduce the vibration of the ground surface along the tunnel without compromising the accepted transportation speed. This can help to mitigate the negative effects that ground vibrations have on the seismic stability of nearby buildings and structures.

3. METHODS

The study presented in this paper employs the mathematical modeling approach based on the theory of elasticity [2]. The tunnel is represented as an infinitely long, circular, cylindrical, three-layer elastic shell situated in a homogeneous, isotropic, and linearly elastic half-space that is parallel to its horizontal boundary. Initially, the load, which moves uniformly with subsonic velocity along the inner surface of the shell, is assumed to be sinusoidal along the shell axis with an arbitrary dependence on the angular coordinate. In order to address the issue, the method of incomplete separation of variables [5–9, 18] is put forth as a potential solution. The solution for the Lamé potentials is presented as a superposition of Fourier-Bessel series and Fourier-type contour integrals. Furthermore, the method of decomposition of potentials into plane waves and decomposition of plane waves into series on cylindrical functions is employed [8, 9, 18]. Subsequently, the solution obtained is employed to solve the problem of the impact of an aperiodic moving load of arbitrary type on the given shell.

4. RESULTS

4.1 Formulation and Analytical Solution of the Problem

Figure 1 depicts the design scheme of a three-layer tunnel with a depth of h , supported by a three-layer lining in a homogeneous and isotropic medium (body). This body is a linear-elastic half-space, as defined by the fixed Cartesian x, y, z and cylindrical

r, θ, z coordinate systems. The z -axis is aligned with the shell axis, while the x -axis is perpendicular to the boundary of the half-space (ground surface). The outermost thin layers of the shell (cladding) with radii of the medial surfaces R_1 and R_2 and thicknesses h_{01} and h_{02} are rigidly coupled with the middle thick layer (filler) and the surrounding elastic medium. Given the thinness of the lining layers, it is reasonable to assume that they are in contact with the filler and the surrounding body along their medial surfaces.

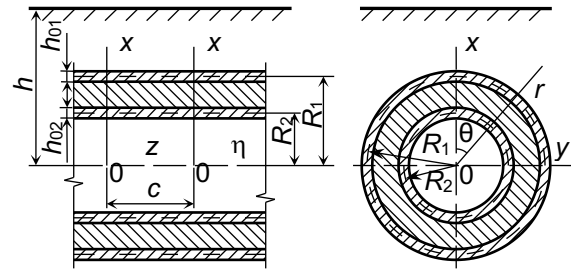


Fig. 1. A three-layer shell in an elastic half-space

The physical and mechanical properties of the materials comprising the shell filler and the surrounding body are characterized by the following constants: ν_k – Poisson’s ratio, μ_k – shear modulus, ρ_k – density ($k = 1, 2$), where index $k = 1$ refers to the body, $k = 2$ – to the shell filler. In regard to the physical and mechanical characteristics of the materials constituting the shell lining layers, the following designations are employed: ν_{0k} – Poisson’s ratio, μ_{0k} – shear modulus, ρ_{0k} – density ($k = 1, 2$). Here the index $k = 1$ refers to the outer lining layer, and $k = 2$ – to its inner layer.

A load of intensity P moves along the inner surface of the shell in the direction of the z -axis with a constant velocity c (less than the velocities of shear wave propagation in the shell filler and the surrounding body).

Since a steady-state process is under consideration, it is appropriate to employ the moving Cartesian $(x, y, \eta = z - ct)$ and cylindrical $(r, \theta, \eta = z - ct)$ coordinate systems (Fig. 1), which move together with the loads.

To describe the motion of the outer layer ($k = 1$) and the inner layer ($k = 2$) of the shell cladding, it is necessary to employ the classical equations of shell theory. In the moving coordinate system, these equations take the form [5]

$$\left[1 - \frac{(1 - \nu_{0k}) \rho_{0k} c^2}{2\mu_{0k}} \right] \frac{\partial^2 u_{0nk}}{\partial \eta^2} + \frac{1 - \nu_{0k}}{2R_k^2} \frac{\partial^2 u_{0nk}}{\partial \theta^2} + \frac{1 + \nu_{0k}}{2R_k} \frac{\partial^2 u_{0nk}}{\partial \eta \partial \theta} + \frac{\nu_{0k}}{R_k} \frac{\partial u_{0rk}}{\partial \eta} = \frac{1 - \nu_{0k}}{2\mu_{0k} h_{0k}} (q_{nk} - q_{\eta Rk}),$$

$$\begin{aligned}
 & \frac{1 + \nu_{0k}}{2R_k} \frac{\partial^2 u_{0\eta k}}{\partial \eta \partial \theta} + \frac{(1 - \nu_{0k})}{2} \left(1 - \frac{\rho_{0k} c^2}{\mu_{0k}} \right) \frac{\partial^2 u_{0\theta k}}{\partial \eta^2} + \\
 & + \frac{1}{R_k^2} \frac{\partial^2 u_{0\theta k}}{\partial \theta^2} + \frac{1}{R_k^2} \frac{\partial u_{0rk}}{\partial \theta} = \frac{1 - \nu_{0k}}{2\mu_{0k} h_{0k}} (q_{\theta k} - q_{\theta Rk}), \quad (1) \\
 & \frac{\nu_{0k}}{R_k} \frac{\partial u_{0\eta k}}{\partial \eta} + \frac{1}{R_k^2} \frac{\partial u_{0\theta k}}{\partial \theta} + \frac{h_{0k}^2}{12} \nabla^2 \nabla^2 u_{0rk} + \frac{u_{0rk}}{R_k^2} + \\
 & + \frac{(1 - \nu_{0k}) \rho_{0k} c^2}{2\mu_{0k}} \frac{\partial^2 u_{0rk}}{\partial \eta^2} = - \frac{1 - \nu_{0k}}{2\mu_{0k} h_{0k}} (q_{rk} - q_{rRk}),
 \end{aligned}$$

where u_{0jk} are the components of displacement of the points of the median surfaces of the shell lining layers; $q_{jR2} = \sigma_{rj2}$ ($r = R_2$), $q_{j1} = \sigma_{rj2}$ ($r = R_1$), $q_{jR1} = \sigma_{rj1}$ ($r = R_1$) are the components of the reaction of the shell filler and the body; σ_{rj1} , σ_{rj2} are the components of stress tensors in the body and shell filler; $q_{j2} = P_j(\theta, \eta)$; $P_j(\theta, \eta)$ are the components of the load intensity $P(\theta, \eta)$; $j = \eta, \theta, r$.

The motion of the body ($k = 1$) and the shell filler ($k = 2$) will be described by the dynamic equations of elasticity theory in vector form presented in the moving coordinate system [5 – 7, 9, 18]

$$(M_{pk}^{-2} - M_{sk}^{-2}) \text{grad div } \mathbf{u}_k + M_{sk}^{-2} \nabla^2 \mathbf{u}_k = \partial^2 \mathbf{u}_k / \partial \eta^2, \quad (2)$$

where $M_{pk} = c/c_{pk}$, $M_{sk} = c/c_{sk}$; $c_{pk} = \sqrt{(\lambda_k + 2\mu_k)/\rho_k}$, $c_{sk} = \sqrt{\mu_k/\rho_k}$ are dilation-compression and shear wave propagation velocities, $\lambda_k = 2\mu_k \nu_k / (1 - 2\nu_k)$, ∇^2 – Laplace operator, \mathbf{u}_k – point displacement vectors.

If the vectors \mathbf{u}_k are expressed in terms of the Lamé potentials φ_{jk} ($j = 1, 2, 3$, $k = 1, 2$) [5 – 7, 9, 18]

$$\mathbf{u}_k = \text{grad } \varphi_{1k} + \text{rot}(\varphi_{2k} \mathbf{e}_\eta) + \text{rot rot}(\varphi_{3k} \mathbf{e}_\eta), \quad (3)$$

it follows from (2) and (3) that φ_{jk} satisfy the equations

$$\nabla^2 \varphi_{jk} = M_{jk}^{-2} \partial^2 \varphi_{jk} / \partial \eta^2, \quad j = 1, 2, 3, \quad k = 1, 2. \quad (4)$$

Here \mathbf{e}_η is the unit vector of the η -axis, $M_{1k} = M_{pk}$, $M_{2k} = M_{3k} = M_{sk}$.

The potentials φ_{jk} are employed to express the components of the stress tensors σ_{lmk} in the body ($k = 1$) and the shell filler ($k = 2$), which are related to the components u_{lk} of the displacement vectors \mathbf{u}_k by Hooke's law ($l, m = r, \theta, \eta$, $k = 1, 2$; $l, m = x, y, \eta$, $k = 1$).

Thus, to determine the SSS components of the body and the shell filler it is necessary to solve

Eqs. (4) in accordance with the following boundary conditions:

$$\text{- when } x = h \quad \sigma_{xx1} = \sigma_{yy1} = \sigma_{xy1} = 0; \quad (5)$$

$$\text{- when } r = R_1 \quad u_{j1} = u_{j2}, \quad u_{j1} = u_{0j1}, \quad (6)$$

$$\text{- when } r = R_2 \quad u_{j2} = u_{0j2}, \quad j = r, \theta, \eta.$$

We will first examine the impact of a load moving sinusoidally with respect to η on the shell

$$P(\theta, \eta) = p(\theta) e^{i\xi \eta}, \quad p(\theta) = \sum_{n=-\infty}^{\infty} P_n e^{in\theta}, \quad (7)$$

$$P_j(\theta, \eta) = p_j(\theta) e^{i\xi \eta}, \quad p_j(\theta) = \sum_{n=-\infty}^{\infty} P_{nj} e^{in\theta}, \quad j = r, \theta, \eta.$$

In a steady state, the dependence of all variables on η has the form (7), thus

$$u_{0jk}(\theta, \eta) = \sum_{n=-\infty}^{\infty} u_{0nj} e^{in\theta} e^{i\xi \eta}, \quad j = r, \theta, \eta, \quad k = 1, 2, \quad (8)$$

$$\varphi_{jk}(r, \theta, \eta) = \Phi_{jk}(r, \theta) e^{i\xi \eta}, \quad j = 1, 2, 3, \quad k = 1, 2. \quad (9)$$

Substituting (9) into (4), we obtain

$$\nabla_2^2 \Phi_{jk} - m_{jk}^2 \xi^2 \Phi_{jk} = 0, \quad j = 1, 2, 3, \quad k = 1, 2, \quad (10)$$

where $m_{jk} = \sqrt{1 - M_{jk}^2}$, $m_{1k} = m_{pk}$, $m_{2k} = m_{3k} = m_{sk}$, ∇_2^2 – two-dimensional Laplace operator.

By employing the (9), we can derive expressions for displacements u_{jk}^* and stresses σ_{lmk}^* ($l, m = r, \theta, \eta$) within the body ($k = 1$) and shell filler ($k = 2$), as well as u_{j1}^* , σ_{lm1}^* ($l, m = x, y, \eta$) within the body, in response to a sinusoidal load (7) as a function of the Φ_{jk} (* means that these components correspond to the case of a sinusoidal moving load (7) affecting the shell).

Since $c < c_{sk}$, $M_{sk} < 1$ ($k = 1, 2$) and the solutions of Eqs. (10) can be formulated as [18]

$$\Phi_{jk} = \Phi_{jk}^{(1)} + \Phi_{jk}^{(2)}, \quad j = 1, 2, 3, \quad k = 1, 2, \quad (11)$$

where:

- for the body

$$\Phi_{j1}^{(1)} = \sum_{n=-\infty}^{\infty} a_{nj} K_n(k_{j1} r) e^{in\theta},$$

$$\Phi_{j1}^{(2)} = \int_{-\infty}^{\infty} g_j(\xi, \zeta) \exp(iy\zeta + (x-h)\sqrt{\zeta^2 + k_{j1}^2}) d\zeta;$$

- for the shell filler

$$\Phi_{j2}^{(1)} = \sum_{n=-\infty}^{\infty} a_{nj+3} K_n(k_{j2} r) e^{in\theta},$$

$$\Phi_{j2}^{(2)} = \sum_{n=-\infty}^{\infty} a_{nj+6} I_n(k_{j2} r) e^{in\theta}.$$

Here, $K_n(k_j r)$, $I_n(k_j r)$ – Macdonald functions and modified Bessel functions, $k_{j1} = |m_{j1} \xi|$, $k_{j2} = |m_{j2} \xi|$; a_{n1}, \dots, a_{n9} , $g_j(\xi, \zeta)$ are unknown coefficients and functions, $j = 1, 2, 3$.

In the Cartesian coordinate system, the expressions for the potentials Φ_{j1} (11) will take the form [18]

$$\Phi_{j1} = \int_{-\infty}^{\infty} \left[\frac{e^{-xf_j}}{2f_j} \sum_{n=-\infty}^{\infty} a_{nj} \Phi_{nj} + g_j(\xi, \zeta) e^{(x-h)f_j} \right] e^{iy\zeta} d\zeta, \quad (12)$$

where

$$f_j = \sqrt{\zeta^2 + k_{j1}^2}, \quad \Phi_{nj} = \left[(\zeta + f_j) / k_{j1} \right]^n, \quad j = 1, 2, 3.$$

From the boundary conditions (5) rewritten for σ_{xmi}^* ($m = x, y, \eta$), using (12), we express the functions $g_j(\xi, \zeta)$ through the coefficients a_{nj} ($j = 1, 2, 3$). By extracting the coefficients at $e^{iy\zeta}$ and equating them to zero, we obtain a system of three algebraic equations, from which we find

$$g_j(\xi, \zeta) = \frac{1}{\Delta_*} \sum_{l=1}^3 \Delta_{jl}^* e^{-hf_l} \sum_{n=-\infty}^{\infty} a_{nl} \Phi_{nl}. \quad (13)$$

The form of determinants Δ_* and Δ_{jl}^* coincides with similar determinants in the case of an unsupported cavity in an elastic half-space and is defined in [8], where it is proved that $\Delta_*(\xi, \zeta)$ does not approach zero if $c < c_R$, where c_R is the velocity of Rayleigh surface waves in the half-space [20].

When $c < c_R$, the relations (12), considering (13), will take the following form

$$\Phi_{j1} = \int_{-\infty}^{\infty} \left[\frac{e^{-xf_j}}{2f_j} \sum_{n=-\infty}^{\infty} a_{nj} \Phi_{nj} + e^{(x-h)f_j} \sum_{l=1}^3 \frac{\Delta_{jl}^*}{\Delta_*} e^{-hf_l} \sum_{n=-\infty}^{\infty} a_{nl} \Phi_{nl} \right] e^{iy\zeta} d\zeta.$$

In the cylindrical coordinate system, when $c < c_R$, the expressions for the potentials Φ_{j1} (11), considering (13), will take the form [18]

$$\Phi_{j1} = \sum_{n=-\infty}^{\infty} (a_{nj} K_n(k_{j1} r) + b_{nj} I_n(k_{j1} r)) e^{in\theta},$$

where $A_{nj}^{ml} = \int_{-\infty}^{\infty} \frac{\Delta_{jl}^*}{\Delta_*} \Phi_{ml} \Phi_{nj} e^{-h(f_l + f_j)} d\zeta,$

$$b_{nj} = \sum_{l=1}^3 \sum_{m=-\infty}^{\infty} a_{ml} A_{nj}^{ml}.$$

Let us substitute the relations found in the cylindrical coordinate system for the potentials Φ_{jK}

into the expressions for displacements u_{ik}^* and stresses σ_{lmk}^* ($l, m = r, \theta, \eta$) in the body ($k = 1$) and shell filler ($k = 2$). Then only the coefficients a_{n1}, \dots, a_{n9} are unknown in these expressions.

By substituting (8) into (1) and solving the resulting system of equations for the n -th term of the expansion with respect to $u_{0m\eta k}$, $u_{0n\theta k}$, and u_{0nrk} , one can obtain the expressions for these variables, which are presented in [5].

To determine the coefficients a_{n1}, \dots, a_{n9} , it is necessary to employ the boundary conditions (6), which have been rewritten for u_{ik}^* ($l = r, \theta, \eta$; $k = 1, 2$).

By substituting the corresponding expressions into (6) and equating the coefficients of the Fourier-Bessel series when $e^{in\theta}$, an infinite system of linear algebraic equations ($n = 0, \pm 1, \pm 2, \dots$) is obtained. The system can be solved using the method of reduction or the method of successive reflections [8], which is more convenient for solving the problem at each successive reflection. This method allows the solution of a system of linear equations of block-diagonal form with matrices of size 9×9 and determinants $\Delta_n(\xi, c)$ along the main diagonal.

When a uniformly moving aperiodic load of the form $P(\theta, \eta) = p(\theta)p(\eta)$ (which is typical for vehicles) affects the shell, it is expressed, as well as the SSS components of the body and the shell filler, in the form of Fourier integrals

$$\begin{aligned} P(\theta, \eta) &= \frac{1}{2\pi} \int_{-\infty}^{\infty} P^*(\theta, \xi) e^{i\xi\eta} d\xi = p(\theta)p(\eta) = \\ &= p(\theta) \frac{1}{2\pi} \int_{-\infty}^{\infty} p^*(\xi) e^{i\xi\eta} d\xi, \\ P_m(\theta, \eta) &= \frac{1}{2\pi} \int_{-\infty}^{\infty} P_m^*(\theta, \xi) e^{i\xi\eta} d\xi = p_m(\theta)p(\eta) = \\ &= p_m(\theta) \frac{1}{2\pi} \int_{-\infty}^{\infty} p^*(\xi) e^{i\xi\eta} d\xi; \\ u_{ik}(r, \theta, \eta) &= \frac{1}{2\pi} \int_{-\infty}^{\infty} u_{ik}^*(r, \theta, \xi) p^*(\xi) d\xi, \\ \sigma_{lmk}(r, \theta, \eta) &= \frac{1}{2\pi} \int_{-\infty}^{\infty} \sigma_{lmk}^*(r, \theta, \xi) p^*(\xi) d\xi. \end{aligned} \quad (14)$$

Here $l = r, \theta, \eta$, $m = r, \theta, \eta$, $k = 1, 2$;

$$p^*(\xi) = \int_{-\infty}^{\infty} p(\eta) e^{-i\xi\eta} d\eta.$$

Any numerical integration method can be employed to calculate displacements and stresses (14) if for each value of $n = 0, \pm 1, \pm 2, \dots$ $\Delta_n(\xi, c) \neq 0$. As shown by the studies of the determinants $\Delta_n(\xi, c)$, it is sufficient for this to happen if the velocity of the loads is less than its

critical velocities $c_{(n)^*}$ ($c < c_{(n)^*}$), which may be less than the Rayleigh velocity of the surface waves. The values of $c_{(n)^*}$ depend on the number n and are determined from the dispersion equations $\Delta_n(\xi, c) = 0$ as minima of the dispersion curves corresponding to these equations from $c \sim \xi$. Furthermore, the minimum critical velocity is observed to occur when $n = 0$ ($\min c_{(n)^*} = c_{(0)^*}$) [8].

4.2 Numerical Experiments

We will consider a tunnel supported by a three-layer steel-concrete lining with a depth of embedment $h = 6$ m in a rock body with the following characteristics: $\rho_1 = 1.5 \cdot 10^3$ kg/m³, $\nu_1 = 0.294$, $\mu_1 = \mu = 1.0935 \cdot 10^8$ Pa. The calculation parameters for the tunnel lining are as follows: the middle layer (filler) is concrete ($\rho_2 = 2.5 \cdot 10^3$ kg/m³, $\nu_2 = 0.2$, $\mu_2 = 1.21 \cdot 10^{10}$ Pa [21]) shell with surface radii $R_1 = 3.0$ m, $R_2 = R = 2.5$ m; the outermost layers (cladding) are thin-walled steel shells ($\nu_{01} = \nu_{02} = 0.3$, $\mu_{01} = \mu_{02} = 8.08 \cdot 10^{10}$ Pa, $\rho_{01} = \rho_{02} = 7.8 \cdot 10^3$ kg/m³). The thickness of the shells is $h_{01} = h_{02} = 0.02$ m.

The transport normal loads of intensity P_r , shown in Fig. 2, move along the tunnel with velocity $c = 100$ m/s. The loads are uniformly distributed along the η axis in the interval $|\eta| \leq l_0 = 0.2$ m.

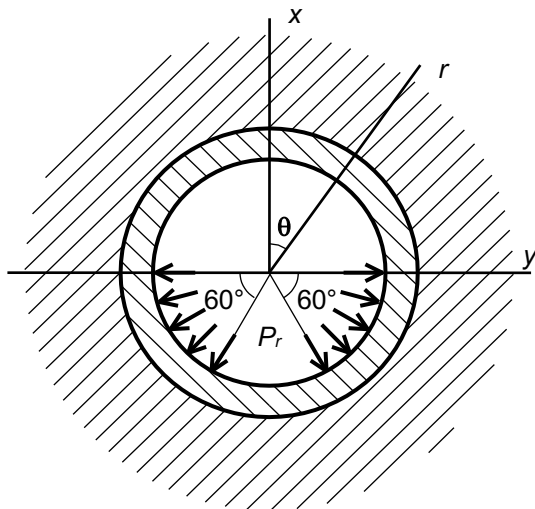


Fig. 2. A load moving through the tunnel

Two cases of tunnel loading will be considered: symmetric and asymmetric.

In the first case, it will be assumed that the load intensity is constant over the entire surface of its application, i.e. $P_r = P^{\circ}$ (Pa).

In the second case, the intensity of the load is uniformly distributed along the angular coordinate to the left of the vertical diametral plane of the tunnel and is therefore twice the intensity of the same load applied to the right of this plane, i.e. when $90^{\circ} \leq \theta \leq 150^{\circ}$ $P_r = P^{\circ}$; when $210^{\circ} \leq \theta \leq 270^{\circ}$ $P_r = 2P^{\circ}$.

The numerical studies of the dispersion equations corresponding to this case have demonstrated that there are no critical velocities within the subsonic velocity range of the load.

The following notations will be introduced (index $k = 1$ in the displacements and stresses designations is omitted): $u^{\circ}_x = u_x \mu / P^{\circ}$ (m), $u^{\circ}_y = u_y \mu / P^{\circ}$ (m), $\sigma^{\circ}_{yy} = \sigma_{yy} / P^{\circ}$, $\sigma^{\circ}_{\eta\eta} = \sigma_{\eta\eta} / P^{\circ}$.

Tables 1 and 2 present the results of calculating the SSS of the ground surface ($x = h$) in the xy ($\eta = 0$) coordinate plane, when the tunnel is loaded with both symmetric and asymmetric transport normal loads. According to the data in Tables 1 and 2, the curves for the variations of u°_x , u°_y , σ°_{yy} , $\sigma^{\circ}_{\eta\eta}$ of the ground surface in the xy -coordinate plane are presented in Figures 3 – 6. The first set of curves (Curves 1) correspond to the case of symmetric loading of the tunnel by transport loads, while the second set of curves (Curves 2) correspond to the case of asymmetric loading.

Table 1. The SSS components of the ground surface in the xy coordinate plane when the tunnel is loaded with symmetric transport normal loads

Comp. SSS	y/R								
	0.0	-0.2	-0.4	-0.6	-0.8	-1.0	-1.2	-1.4	-1.6
$u^{\circ}_x \times 100$	-0.96	-0.96	-0.92	-0.92	-0.92	-0.88	-0.88	-0.84	-0.84
$u^{\circ}_y \times 10^3$	0.0	0.16	0.28	0.36	0.44	0.48	0.48	0.44	0.40
$\sigma^{\circ}_{yy} \times 10^3$	-1.68	-1.64	-1.48	-1.28	-1.04	-0.80	-0.60	-0.44	-0.32
$\sigma^{\circ}_{\eta\eta} \times 10^3$	-3.20	-3.16	-3.04	-2.88	-2.72	-2.52	-2.32	-2.16	-2.04

Table 2. The SSS components of the ground surface in the xy coordinate plane when the tunnel is loaded with asymmetric transport normal loads

Comp. SSS	y/R								
	0,0	-0.2	-0.4	-0.6	-0.8	-1.0	-1.2	-1.4	-1.6
$u^{\circ}_x \times 100$	-1.44	-1.44	-1.44	-1.44	-1.40	-1.36	-1.32	-1.32	-1.28
$u^{\circ}_y \times 100$	-0,68	-0.68	-0.64	-0.60	-0.60	-0.56	-0.56	-0.56	-0.56
$\sigma^{\circ}_{yy} \times 10^3$	-2,68	-2.84	-2.80	-2.56	-2.20	-1.76	-1.32	-0.92	-0.60
$\sigma^{\circ}_{\eta\eta} \times 10^3$	-4,88	-4.96	-4.88	-4.72	-4.44	-4.12	-3.80	-3.48	-3.20

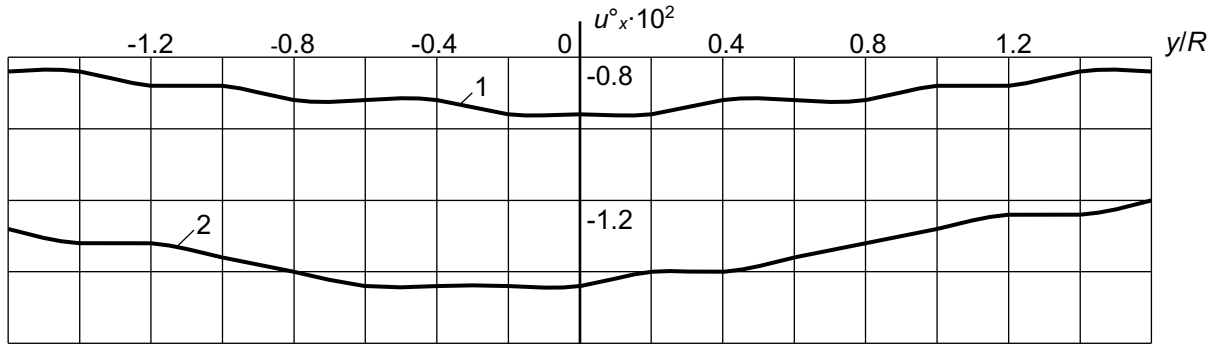


Fig. 3. Displacements u_x of the ground surface in the xy coordinate plane

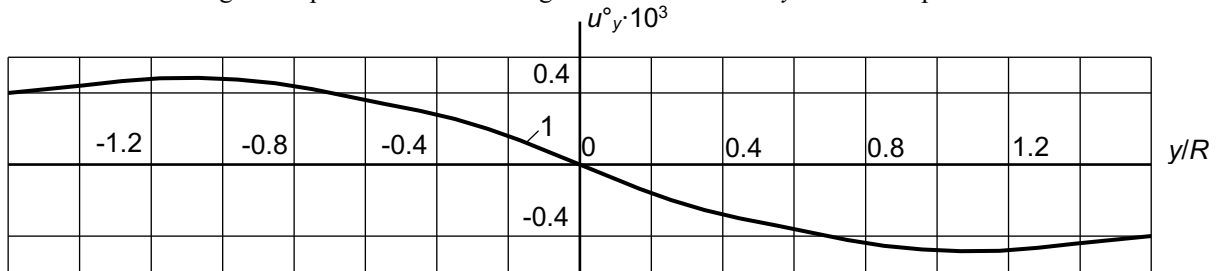


Fig. 4. Displacements u_y of the ground surface in the xy coordinate plane

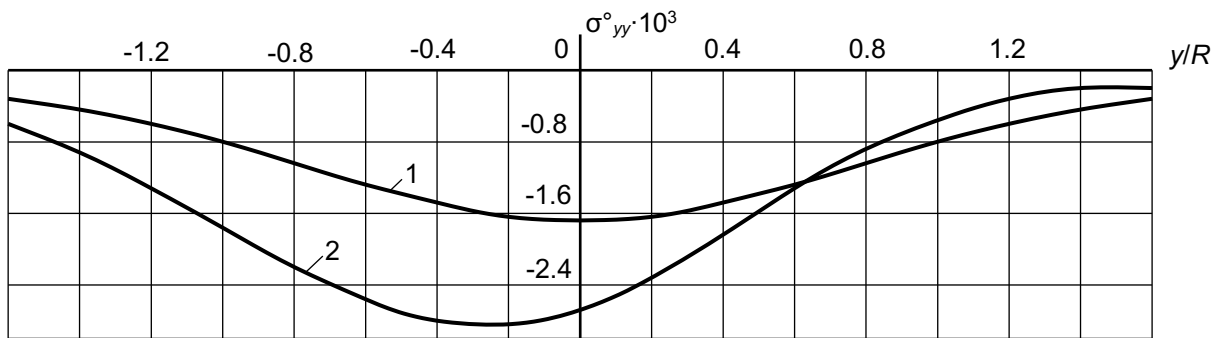


Fig. 5. Stresses σ_{yy} of the ground surface in the xy coordinate plane

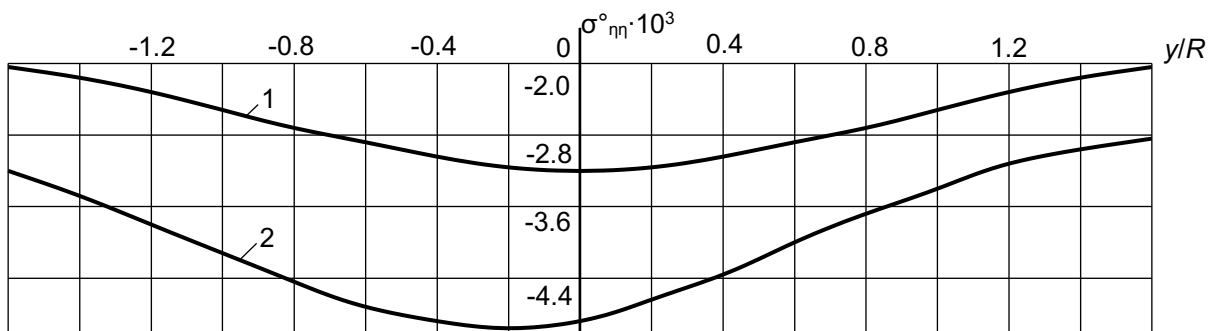


Fig. 6. Stresses $\sigma_{\eta\eta}$ of the ground surface in the xy coordinate plane

5. DISCUSSION

The analysis of the calculation results reveals that vertical displacements of the u_x points (deflections) of the ground surface occur in a

downward direction (in the direction of the symmetrical transport loads or the vertical component of the asymmetrical transport loads). Furthermore, the stresses σ_{yy} and $\sigma_{\eta\eta}$ in these points are compressive (Fig. 3, 5, 6). When the tunnel is

loaded with symmetrical transport loads, the curves of changes u_x^0 , σ_{yy}^0 , $\sigma_{\eta\eta}^0$ of the ground surface exhibit a symmetrical pattern with respect to the x -axis, reaching their maximum values when $y = 0$. That is, at $y = 0$ $|u_x| = \max|u_x|$, $|\sigma_{yy}| = \max|\sigma_{yy}|$, $|\sigma_{\eta\eta}| = \max|\sigma_{\eta\eta}|$. As the value of $|y|$ increases, the values of $|u_x|$, $|\sigma_{\eta\eta}|$, $|\sigma_{yy}|$ decrease. In the case of asymmetric transport load (when the intensity of the left half of the symmetrical transport load increases twice), the symmetrical nature of the ground surface variation curves u_x^0 , σ_{yy}^0 , $\sigma_{\eta\eta}^0$ is disrupted. The largest deflection increases by 1.5 times, $\max|\sigma_{\eta\eta}|$ by 1.55 times ($y = -0.2R$), and $\max|\sigma_{yy}|$ by 1.69 times ($y = -0.2R$). It is important to note that when the intensity of a symmetric load is increased by a factor of 1.5, that is when its resultant is equal to the vertical component of the resultant of the asymmetrical load, the values of components of the ground surface SSS u_x , u_y , σ_{yy} , $\sigma_{\eta\eta}$ will also increase by a factor of 1.5.

As follows from Fig. 4, when the tunnel is subjected to a symmetric transportation load, the horizontal displacements of the u_y points (shears) of the ground surface, when $y < 0$, occur to the right, and when $y > 0$, they occur to the left (when $y = 0$, $u_y = 0$). Symmetric points relative to the x -axis exhibit the same displacement. As $|y|$ increases from 0 to $1.1R$, the values of $|u_y|$ increase (at $|y| = 1.1R$ $|u_y| = \max|u_y|$). However, as $|y|$ continues to increase, the values of $|u_y|$ begin to decrease. In the case of an asymmetric transport load (with the intensity of the left half of the symmetric transport load doubled), horizontal displacements u_y of all points on the ground surface occur to the left (in the direction of the horizontal component of the resultant of this load), and $\max|u_y|$ increases by a factor of 15 (Table 2).

6. CONCLUSION

A model problem is solved to study the dynamics of a shallow tunnel supported by a three-layer lining under steady-state transport loads. Unlike similar works, where the rock body is represented as an elastic space, this paper provides it as an elastic half-space.

The authors conducted numerical experiments using developed computer programs to examine two scenarios of loading a shallow tunnel supported by a three-layer steel-concrete lining (comprising a thick middle concrete layer and thin outer steel layers) with a uniform, normal load moving along its lower half. The loading was considered both symmetric with respect to the vertical diametral plane of the tunnel and asymmetric. The numerical values of the SSS components of the ground surface in the plane normal to the tunnel axis, passing through the centre

of the moving load, were obtained. The results of the calculation are subjected to analysis, which reveals that as the intensity of the half-symmetric load increases, the nature of the changes in displacements and stresses on the ground surface undergoes a transformation, with their extreme values also demonstrating a corresponding increase. The most notable increase is observed in the horizontal displacements. It is, therefore, necessary to ensure that the transport loads in the tunnel have a symmetric form relative to its vertical diametral plane in order to avoid unacceptable displacement of the ground surface during the operation of a shallow tunnel in urban development conditions.

The mathematical model of the dynamics of a shallow tunnel supported by a three-layer lining under transport loads, developed and presented in this paper can be utilized by design engineering organizations with a specialization in the field of metro and tunnel engineering.

It should be noted that the obtained solution can only be applied in the case of thin shell linings, for which the classical equations of shell theory are valid in describing their motion. Otherwise, their motion should be described by the dynamic equations of elasticity theory, which defines the direction for future research.

7. REFERENCES

- [1] Sheng X., A Review on Modelling Ground Vibrations Generated by Underground Trains, International Journal of Rail Transportation, Vol. 7, No. 4, 2019, pp. 241-261.
- [2] Yerzhanov Zh.S. and Aitaliev Sh.M., The dynamics of tunnels and underground pipelines, Nauka, Alma-Ata, 1989, pp. 1-240.
- [3] Lvovsky V.M., Steady-state oscillations of a cylindrical shell in an elastic medium under the action of a moving load, *Sat.: Issues of strength and ductility*, Dnipropetrovsk, 1974, pp. 98-110.
- [4] Pozhuev V.I., The action of moving load on a cylindrical shell in an elastic medium, *Structural Mechanics and Structural Analysis*, No. 1, 1978, pp. 44-48.
- [5] Alexeyeva L.A. and Girnis S.R., Research of dynamic behaviour of trilaminar casing in elastic space at influence of moving loading, *Mathematical journal*, Vol. 9, No. 4, 2009, pp. 5-13.
- [6] Otarbaev Zh.O., Influence of contact conditions on two-layer shell a tunnel of a deep embedding and a massif on its tense-deformed condition at action of transport loads, *Vestnik KazNTU*, No. 2, 2015, pp. 274-280.
- [7] Bulyga L.L. and Stanevich V.T., Action of Moving Load on a Two-Layer Shell in Elastic Medium, *Lecture Notes in Networks and Systems*, Vol. 574, 2023, pp. 2301-2311.

- [8] Alekseeva L.A. and Ukrainets V.N., Dynamics of an elastic half-space with a reinforced cylindrical cavity under moving loads, *International Applied Mechanics*, Vol. 45, Issue 9, 2009, pp. 75-85.
- [9] Alexeyeva L.A., Model of the dynamics of a tunnel and a shallow underground pipeline under the action of traffic loads, *Bulletin of L.N. Gumilyov ENU, Mathematics. Computer science. Mechanics series*, Vol. 133, No. 4, 2020, pp. 28–39.
- [10] Otarbaev Zh.O., Influence of friction during transportation of loads through underground pipelines on the stress-deformed state of the earth surface, *Bulletin of Kazakh Leading Academy of Architecture and Construction*, No. 1, 2022, pp. 189-198.
- [11] Gorshkova L. and Zhukonova G., The impact of normal and tangential loads on a shallow tunnel, *Bulletin of L.N. Gumilyov ENU, Mathematics. Computer science. Mechanics series*, Vol. 144, No. 3, 2023, pp. 12-22.
- [12] Makashev K.T. and Stanevich V.T., Dynamic response of unsupported and supported cavities in an elastic half-space under moving normal and torsional loads, *Bulletin of the Karaganda University, series Physics*, Vol. 112, No. 4, 2023, pp. 65-75
- [13] Yuan Z., Boström A., Cai Y. and Cao Z., Closed-Form Analytical Solution for Vibrations from a Tunnel Embedded in a Saturated Poroelastic Half-Space, *Journal of Engineering Mechanics*, Vol. 387, 2017, pp. 177-193.
- [14] Boström A. and Yuan Z., Benchmark solutions for vibrations from a moving source in a tunnel in a half-space, *In Ground Vibrations from High-Speed Railways*, ICE Publishing, 2019, pp. 261-281.
- [15] Coşkun İ. and Dolmaseven D., Dynamic Response of a Circular Tunnel in an Elastic Half Space, *Journal of Engineering*, Hindawi Limited, Vol. 2017, 2017, pp 1-12.
- [16] He C., Zhou S., Di H., Guo P. and Xiao J., Analytical method for calculation of ground vibration from a tunnel embedded in a multi-layered half-space, *Computers and Geotechnics*, Vol. 99, 2018, pp. 149-164.
- [17] He C., Jia Y. and Zhou S., Semi-analytical method for calculating ground vibrations from a tunnel in a homogeneous half-space with an irregular surface, *Journal of Sound and Vibration*, Vol. 591, 2014, pp. 118-615.
- [18] Girmis S., Ukrainets V., Stanevich V., Gorshkova L. and Akhmetova A., The Transport Load Influence on a Reinforced Two-Layered Tunnel Lining, *International Journal of GEOMATE*, Vol. 26, Issue 117, 2024, pp. 27-34.
- [19] Liu X., Liu Y., Jiang Z., Wang J. and Mang H. A., Numerical investigation of the mechanical behavior of segmental tunnel linings reinforced by a steel plate – Concrete composite structure, *Engineering Structures*, Vol. 276, No. 3, 2023, pp. 115-130.
- [20] Novackij V., *Theory of elasticity*, Mir, Moscow, 1975, pp. 1-872.
- [21] Rakhimov M.A., Rakhimova G.M. and Suleimbekova Z.A., Modification of Concrete Railway Sleepers and Assessment of Its Bearing Capacity, *International Journal of GEOMATE*, Vol. 20, Issue 77, 2021, pp. 40-48.

Copyright © Int. J. of GEOMATE All rights reserved, including making copies, unless permission is obtained from the copyright proprietors.
